

Altermagnetism in the hopping regime

✉ E.F. Galindez-Ruales, S. Das, ✉ C. Schmitt, ✉ F. Fuhrmann, and ✉ G. Jakob

Institute of Physics, Johannes Gutenberg University Mainz, Staudingerweg 7, 55128 Mainz, Germany.

L. Šmejkal and J. Sinova

*Institute of Physics, Johannes Gutenberg University Mainz, Staudingerweg 7, 55128 Mainz, Germany. and
Institute of Physics, Academy of Sciences of the Czech Republic, 182 00 Prague 8, Czech Republic.*

E. Baek

*Institute of Physics, Johannes Gutenberg University Mainz, Staudingerweg 7, 55128 Mainz, Germany. and
Department of Physics and Chemistry, DGIST, Daegu 42988, Republic of Korea.*

R. González-Hernández

Grupo de Investigación en Física Aplicada, Departamento de Física, Universidad del Norte, Barranquilla, Colombia.

A. Rothschild

*Department of Materials Science and Engineering,
Technion-Israel Institute of Technology, Haifa 32000, Israel.*

C.-Y. You

Department of Physics and Chemistry, DGIST, Daegu 42988, Republic of Korea.

✉ M. Kläui

*Institute of Physics, Johannes Gutenberg University Mainz, Staudingerweg 7, 55128 Mainz, Germany. and
Center for Quantum Spintronics, Norwegian University of Science and Technology, Trondheim 7491, Norway.**

(Dated: January 23, 2024)

Conventional antiferromagnets are known for their time-reversal symmetry in their electronic structure, which results in a zero anomalous Hall coefficient. On the other hand, compensated magnets with noncollinear or canted moments or altermagnets can yield a nonzero anomalous Hall signal and a nondissipative transversal current. While high-symmetry systems typically exhibit an isotropic Hall effect, more interesting are low-symmetry systems, such as hematite, which demonstrates exceptional magnetotransport behavior as it becomes conductive upon slight Ti doping. We scrutinize the magnetotransport in Titanium-doped hematite, revealing a pronounced and unconventional symmetry dependence, particularly contingent on crystal orientation. Our findings establish a compelling correlation between our experimental observations and the classification of hematite as an altermagnet with anisotropic magnetotransport and anomalous Hall effect. Remarkably, our observations result from measurements in the hopping-transport regime, showing that particular transport properties in altermagnets are not limited to conventional band conduction.

Hematite (α -Fe₂O₃) is a well-studied material in the realm of solid-state physics and is renowned for its intricate electronic and magnetic properties. Recently, this topic has garnered substantial attention, particularly in the context of spintronics and other emerging applications [1–10]. Here, we focus on the magnetotransport properties most relevant for spintronics. At temperatures between 960 and 265 K, hematite is a canted antiferromagnet with a weak in-plane ferromagnetic moment (in the hexagonal setting of the rhombohedral space group 167). Below the Morin transition (MT) temperature of $T_M = 265$ K spins reorient to a perfectly compensated collinear antiferromagnetic order along the c -axis. This transition is attributed to the interplay between magnetic dipole and single-ion anisotropy energies [11]. These distinct states, referred to as the weak ferromagnetic (WFM) and collinear antiferromagnetic (AFM) states,

have been extensively investigated with a primary focus on spin transport driven by magnons [5, 12]. Hematite thin films can display altered Morin transition behavior due to growth-induced strain. [5]. Additionally, doping has been used to modulate the properties of hematite, revealing that even minimal dopant percentages can induce changes in magnetic anisotropies and shift the Morin transition temperature without substantially affecting other magnetic properties [13, 14].

A second effect of the doping is that the insulating hematite becomes electrically conducting. However, for samples with high longitudinal resistivity, it was previously not possible to determine a Hall coefficient [15, 16]; heavily doped samples have exhibited more conventional Hall effect behavior, with the Hall voltage directly proportional to the applied field within a specific temperature range [17]. The careful selection of dopants is crucial

for preventing stress and altering hematite properties [13, 14, 18]. Below a 2% doping level, the dopants have been reported to be fully ionized at all temperatures, ensuring a stable carrier concentration with minimal impact on magnetism [19, 20]. The material’s electronic transport properties are accessed by judiciously controlling the doping percentage, leading to a controlled shift in the Fermi level by a few tenths of an electronvolt while retaining the antiferromagnetic characteristics of hematite [21–23].

So far, the particular transport properties of hematite resulting from its particular symmetry have not been explored, while various low symmetry materials have revealed novel Hall effects based on intrinsic spin properties, such as the spin Hall effect, inverse spin Hall effect, or quantum spin Hall effect, [24]. Recent predictions have hinted at novel transport effects in systems with particular symmetries [25, 26], classifying hematite as an altermagnet [27, 28]. However, further work is needed to elucidate its altermagnetic properties in more detail. The Anomalous Hall Effect (AHE), initially explored in ferromagnetic materials, has gained importance in anti-ferromagnetic materials (AFM) [29, 30] and altermagnets [27, 31]. In compensated magnets, the AHE can arise from the induced canted moment during spin reorientation, breaking symmetry and resulting in a nonzero AHE. The structural arrangement and chirality of nonmagnetic atoms can also contribute to the AHE signal [27, 32, 33]. An open question concerns the origin and symmetry of the magnetotransport signals in hematite and the underlying mechanisms, specifically regarding the contribution of the Anomalous Hall Effect (AHE). Thus far, experimental investigations have been limited by the sample geometry, preventing the necessary measurement of the angular dependence required for the symmetry analysis. In particular, this has hindered the ability to relate experimental results to the predicted AHE in altermagnets, which is attributed to the interplay of collinear magnetic order and the particular crystal structure symmetry [27].

In this article, we investigate the anisotropic magnetotransport, including the anomalous Hall effect, in low Ti-doped hematite. By introducing low-level doping, we can access the material’s electronic transport properties. We focus on 1% Ti-doped hematite thin films (150 nm thick), highlighting the intriguing characteristics of the anomalous Hall effect in this system. Our measurements reveal a pronounced sensitivity of the transverse voltage to the crystallographic direction in the ab -plane, including an unexpected sign inversion. The complex signal is in line with the low symmetry responsible for the altermagnetism.

Hematite exhibits a hexagonal crystalline structure (see Fig. 1.a for the rhombohedral primitive unit cell) composed of two sublattices of iron atoms surrounded by oxygen atom cages. Notably, hematite manifests three magnetic phases at varying temperatures, as depicted in

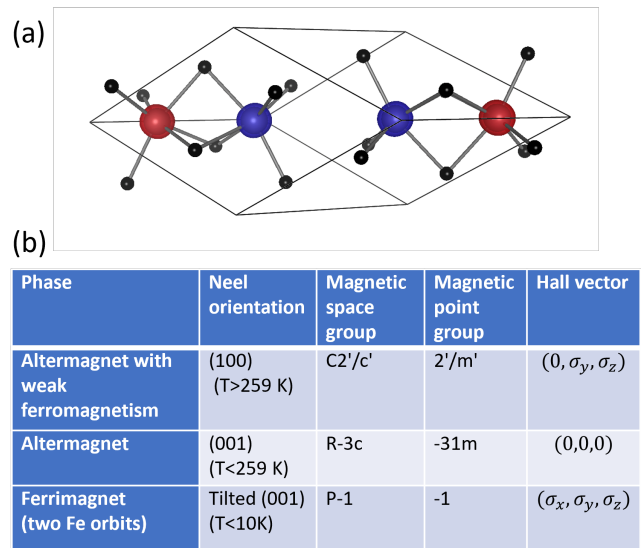


FIG. 1. (a) Visual representation of hematite’s rhombohedral unit cell, showcasing the two iron sublattices (red and blue) and the oxygen atoms (black) in noncentrosymmetric positions. The line along the Fe atoms defines the c -axis using the hexagonal setting of space group 167. The red and blue magnetization isosurfaces are calculated from first-principle calculations in VASP without spin-orbit coupling. (b) The different magnetic phases of hematite, with the corresponding magnetic space and point groups. The Morin temperature characterizes the altermagnetic phases that have, respectively lack weak ferromagnetism, resulting in a nonzero magnetization at high temperatures.

the table in Fig. 1.b. These phases are characterized by their magnetic space and point groups. The atomic rhombohedral space group D_{3d}^6 of hematite is consistent with three possible magnetic point groups corresponding to three possible states. Simultaneously accounting for crystallographic and magnetic groups is the key to understanding hematite symmetries [34].

High-quality films, oriented along (0001), of doped hematite (α - $\text{Fe}_{1.99}\text{Ti}_{0.01}\text{O}_3$: (Ti) α - Fe_2O_3) were deposited onto c -plane sapphire substrates via pulsed laser deposition. Hall bars were meticulously patterned at various in-plane orientations relative to the \mathbf{a} -axis. A comprehensive account of the fabrication procedures and sample quality is provided in the Supplemental Material [35] (see also references [4, 13, 27, 28, 36–42] therein). Magnetization measurements, as illustrated in Figure 2.b, unveil a conspicuous decrease in the magnetic moment below 338 K, unequivocally marking the Morin transition (MT). Notably, this transition exhibits a broader profile compared to single crystals, an observation that we attribute to the presence of a multidomain state within our samples, as expounded upon in the work by Morin et al. [11] and our previous works [4, 5].

Accordingly, the easy-axis phase, showcased in Figure 2.a, did not demonstrate a substantial magnetic moment,

agreeing with typical magnetic properties of hematite. Furthermore, the magnitude of the canted moment of the weak ferromagnetic phase closely corresponds with the bulk values, as corroborated by the references in Lebrun et al. [4], and previous work by Danneger et al. [12]. The absence of secondary phases, the well-defined in-plane orientation, the occurrence of the Morin transition, and the consistency of the canted magnetic moment with established values collectively suggest that the doping level exerts minimal influence on the magnetic properties of hematite.

Determining the conducting regime is a crucial step in selecting the appropriate analytical approach. For our samples with relatively low conductivity, this determination is based on studying resistivity as a function of temperature, as depicted by the blue line in Figure 2.c. While a semiconductor-like model provides a reasonable fit, the derived activation energy of $E_a = 1600k_B \cdot K$ does not correspond to the known gap of hematite. Furthermore, the thermal activation factor value at room temperature ($\exp(-E_a/k_B T) \approx 5 \times 10^{-3}$) strongly suggests that the dominant transport mechanism is characteristic of hopping-like transport. Given the 1% doping in our samples, a substantial number of charge carriers are expected. For Ti, n -doping should occur, yielding a Hall coefficient $R_H = 1/ne \approx -4 \cdot 10^{-6} \text{m}^3/(\text{As})$ in a single band model at room temperature and a corresponding transverse Hall resistance of $25 \Omega/\text{T}$. Notably, a conventional Hall coefficient of approximately $-5 \text{cm}^3\text{C}^{-1}$ is observed over a broad temperature range, as referenced in [17, 20]. While we also observe a Hall voltage of this order of magnitude in the low-field regime, the mean free path for that carrier density in the band conduction regime corresponds to 10^{-12}m . Thus, the most likely scenario is conduction by hopping within the impurity "band" of the donors. Therefore, we cannot directly convert our measured transverse resistivities to Hall conductivities or compare them to the results of band structure calculations, which show spin-polarized conductivity along specific crystal directions for altermagnets [27, 28]. However, we can analyze the directional dependence of our transport experiments. As the band structure is typically solved in reciprocal space, which is nothing other than the Fourier transform of the real space, we expect a directional dependence of hopping processes that mimics the symmetry of the band structure. Notably, an AHE is forbidden in the altermagnetic phase of hematite because spins are (anti)aligned along a high-symmetry direction. However, breaking the symmetry by a high magnetic field that induces a spin flop to a canted antiferromagnetic spin alignment and anomalous Hall components are allowed in the band conductivity. We find a notable increase in our Hall signals in proximity to the spin flop transition, as demonstrated in Figure 3. We demonstrate an unusual directional dependence in our samples' transverse resistivity, which would not be expected for a conventional ferromagnet or a canted

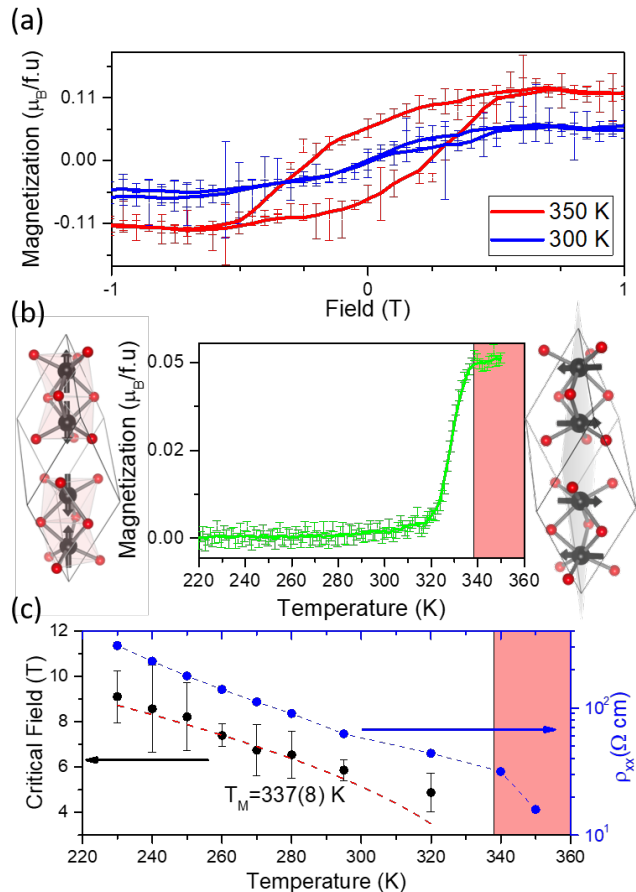


FIG. 2. SQUID magnetometry measurements for a magnetic field applied perpendicular to the c -axis. (a) Magnetization per formula unit as a function of the magnetic field for the Ti-doped samples in both the collinear phase (300 K) and the weak ferromagnetic phase (350 K). At elevated temperatures, the hysteresis loop for the canted moment saturates at $\sim 0.5 \text{ T}$. The small signal observed at lower temperatures is attributed to the nucleation of the $\gamma\text{-Fe}_2\text{O}_3$ phase at the substrate interface. (b) The magnetization as a function of temperature under an external magnetic field of 20 mT reveals an increase in magnetization as temperature increases due to the Morin transition. This transition, from the collinear phase (left panel) to the weak ferromagnetic phase (right panel), occurs over a temperature range of 20 Kelvin. (c) The critical field (H_c) required to reach the spin flop state varies depending on the temperature, while the longitudinal resistivity decreases proportionally. H_c is well described by $H_{cr}(T) \propto \sqrt{T_M - T}$ following the Landau theory, and the resistivity behaves in accordance with transport due to hopping in the impurity band of the donors. The error bars represent the standard error of the measurement (a) or the fitting (c).

antiferromagnet.

The Hall signal within the collinear phase exhibits a minimal response at low magnetic fields, but it undergoes a substantial anomalous change in proximity to the spin-flop transition. This transition involves the rotation of the Néel vector from the out-of-plane (OOP) direc-

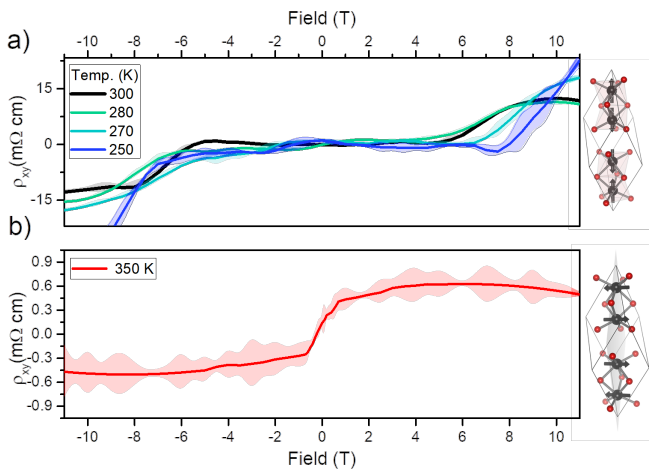


FIG. 3. Hall resistivity in relation to the out-of-plane (OOP) field for temperatures both below (a) and above (b) the Morin transition. The shadow color denotes the standard deviation across 20 different field cycles. The shift in the critical field with temperature in the collinear phase signifies the correspondence between the spin-flop and the Morin transition, as expected for hematite. The magnetic configurations of the iron (Fe) atoms in both phases are depicted on the right side of the graph.

tion into the basal plane, leading to the formation of a canted magnetic moment. The critical field, marking the point at which the transverse resistivity increases, aligns in energy with the Morin transition. This critical field temperature dependence follows a square root relationship, as represented by the red dotted line in Figure 2.c, with a critical temperature (T_M) measured at 337 ± 8 K. This behavior aligns with the characteristics of a typical second-order phase transition as outlined in the Landau theory and is consistent with previous reports [43, 44]. It is important to note that the presence of a multidomain state in our samples results in a different definition of the Morin transition based on this critical temperature. In our context, the critical point is established as the point where the slope deviates from 0, either as dM/dT begins decreasing with temperature (MT) or as $d\rho_{xy}/dH$ starts increasing with the magnetic field (H). The energetically equivalent field-induced spin-flop transition mirrors the alteration in the symmetry of the system observed during the Morin transition. Beyond the spin-flop transition, the Hall vector becomes accessible (see the table in Fig. 1.b), allowing us to explore and measure its properties.

In the high-temperature weak ferromagnetic phase, as depicted in Figure 3.b, the transverse resistivity signal aligns with the anticipated behavior associated with the Anomalous Hall Effect (AHE). It saturates following the canted moment observed in the samples for all investigated Hall bar directions. In this phase, we observe an in-plane anisotropy with a reduced signal amplitude (see supplemental material [35]). Within the collinear phase,

the transverse conductivity signals resulting from the magnetic point group allow for the out-of-plane Hall vector [45]. To understand the relation to the low symmetry crystal structure, we next investigate the dependence of the transverse resistivity with respect to the direction between the current and crystallographic axes. Figure 3 displays the results for current directions along one of the three primary \mathbf{a} -axes, and a fully antisymmetric signal in the transverse conductivity is observed. Essentially, one could understand these signals resulting from the symmetry breaking from reorientation of the moments induced by the field above the spin flop [19]. Any minor hysteresis in the Hall signal could be attributed to potential magnetic domain configurations [5, 13]. The variations in domain size in each structure may result from strain-induced anisotropy introduced during the patterning process [46].

At high fields above the spin-flop field, intriguing phenomena emerge when the Hall bar is patterned at an orientation that deviates from the high-symmetry \mathbf{a} -axis, as illustrated in Fig. 4. Here, we observe transverse signals strongly dependent on the direction of the current flow that do not exhibit purely odd behavior concerning the magnetic field. As the linear resistivity tensor of a hexagonal crystal is isotropic in plane, these signals must be related to the spin structure. The signals differ strongly in rotated Hall bars despite the same canted moment contribution, which is determined by the fixed orientation of the crystal and the external field direction. In less symmetrical orientations (e.g., purple and blue lines), the odd contributions are reduced while strong transverse conductivities evolve that are even with respect to the field direction. These non-Hall-like contributions, stemming from symmetry reduction due to the relative orientation of the injected current and the conductivity tensor, even show a clear sign change (purple line in Fig.4.b).

The odd component of the transverse voltage, associated with the Hall conductivity, mainly displays modulation amplitude that follows a sixfold symmetry that can arise, for instance, from the magnetic anisotropy of hematite [34]. However, looking more closely, the weak odd signal at $+45$ degrees has an inverted sign with respect to the others. Such a sign inversion would not be expected to result from interacting with a positively defined energy landscape of sixfold symmetry. This directional dependence also appears in the components of the transverse conductivity, even with the magnetic field but with inverse magnitude. When the odd signal is strong, the even signal is weak, but the signs of both signals are identical for each individual Hall bar. Importantly, crystallographically equivalent orientations exhibit similar absolute sizes of Hall signals (-45 and $+45$ degrees) or nearly identical signals (-30 and 90 , 0 and 120 degrees), demonstrating that external effects such as differences in the patterning of the structures are not the origin of the observations.

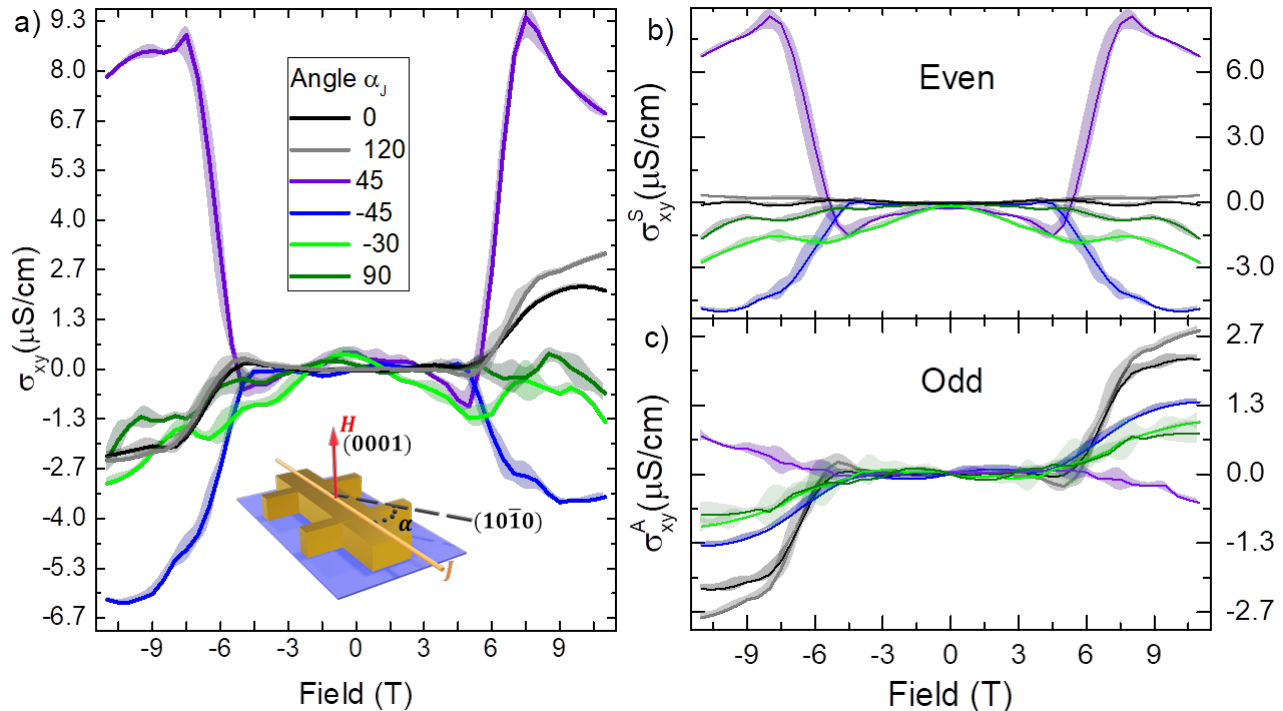


FIG. 4. (a) The transverse conductivity at 300 K of different devices measured at various angles relative to the in-plane crystallographic axis, denoted as \mathbf{a} ($10\bar{1}0$). A diagram illustrating the different device orientations is provided. (b) Even and (c) odd contributions to the Hall conductivity at 300 K from various devices measured at different angles relative to the in-plane crystallographic axis, identified as \mathbf{a} ($01\bar{1}0$). A diagram illustrating the diverse device orientations is provided below. The even contribution displays substantial variations in the weight of the Hall signal across different relative orientations. Simultaneously, the sign inversion observed in the odd portion cannot be attributed to a weak moment-induced anomalous Hall effect contribution. The shadow color indicates the standard deviation based on 20 different field cycles.

Clearly, the crystal symmetry combined with a magnetic order parameter leads to a nondiagonal conductivity tensor of the system. The sign changes along different directions indicate that an order parameter of the system undergoes sign changes depending on the direction. Due to the underlying crystal symmetry, this order parameter must have either 6 or 12 nodes with either maxima or nodes aligned along the crystallographic a -axis. Such an order parameter exists in the underlying altermagnetic phase of hematite (see Supplemental Material [35]).

Anisotropic transport in metallic systems is linked to the crystallographic orientation through the crystal field and spin-orbit interactions [47]. In hopping-like transport, as we observe here, the directionality of hopping is most often neglected. However, hopping processes from one impurity to the next take place in the same crystal potential that provides an altermagnetic band structure, which relates spin-dependent directional transport to orbital alignment in real space. Such an orbital alignment should correspondingly show up in spin-dependent directional hopping probabilities. The fact that hopping processes in poorly conductive ferromagnets can be spin-dependent in a ferromagnet was demonstrated in previous studies

[48, 49]. However, this is not the case for an ordinary compensated magnet, but it could be applicable to an altermagnetic material [27]. Hematite, which is predicted to be an altermagnet material [28], allows for a local magnetization density difference for each sublattice, potentially explaining the Hall sign inversion by reversing local crystal anisotropies (e.g., changing the orientation of the Hall bar) while maintaining fixed sublattice moment directions and Néel vector [45]. However, quantifying the contribution of the altermagnetic properties is challenging from our measurements in our poorly conducting transport regime.

In our samples, which are characterized by a low conductivity regime, hopping transport dominates with a Hall mobility of approximately $0.1 \text{ cm}^2\text{V}^{-1}\text{s}^{-1}$. We successfully measured contributions from different conductivity tensor components despite the limited conductivity. Accessing these terms depends on lowering the system's symmetry, specifically when the current vector deviates from a high symmetry axis. Notably, this orientation-dependent behavior does not depend on the constant canted moments induced during spin reorientation across all device orientations at a fixed field strength. Although

our measurements are within the hopping regime, the magnetic behavior observed in our samples is in line with the characteristic properties of hematite, including the Morin transition, spin-flop transition, and magnitude of the canted moment.

In conclusion, the complex angular dependence of the Hall signal, including the intriguing sign inversion observed in the odd part of the Hall conductivity in hematite, is likely rooted in the distinctive anisotropic altermagnetic properties of the material. This sign inversion unveils unique underlying mechanisms governing the anomalous Hall effect (AHE) in this specific material, adding a layer of complexity to our understanding and showing that even in the hopping regime, transport properties that can be related to altermagnetism can be prominent.

The observed complex symmetry of the Hall signal invites further investigation, especially concerning different doping levels, which, however, extends beyond the scope of our current work. Such research will be pivotal for obtaining a comprehensive understanding of the specific mechanisms responsible for the observed symmetries and the sign inversion in the Hall conductivity.

ACKNOWLEDGMENTS

This work was supported by the Max Planck Graduate Center with the Johannes Gutenberg-Universität Mainz (MPGC). The authors at Mainz acknowledge support from the DFG project number 423441604. All authors from Mainz also acknowledge support from SPIN + X (DFG SFB TRR 173 No. 268565370, projects A01, A03, and B02). M.K. acknowledges support from the Research Council of Norway through its Centers of Excellence funding scheme, project number 262633 "QuSpin." C.-Y.Y. and E.B. acknowledge support from the National Research Foundation of Korea (Grant No. 2021M3F3A2A01037525).

SUPPORTING INFORMATION

Supporting information available on LINK

* klaeui@uni-mainz.de

- [1] V. Baltz, A. Manchon, M. Tsoi, T. Moriyama, T. Ono, and Y. Tserkovnyak, Antiferromagnetic spintronics, *Rev. Mod. Phys.* **90**, 015005 (2018).
- [2] W. R. W. Ahmad, M. H. Mamat, A. S. Zoolfakar, Z. Khusaimi, and M. Rusop, A review on hematite α -Fe₂O₃ focusing on nanostructures, synthesis methods and applications, in *2016 IEEE Student Conference on Research and Development (SCoReD)* (2016) pp. 1–6.
- [3] A. Mirzaei, B. Hashemi, and K. Janghorban, α -Fe₂O₃ based nanomaterials as gas sensors, *J. Mater. Sci. Mater. Electron.* **27**, 3109–3144 (2015).
- [4] R. Lebrun, A. Ross, S. A. Bender, A. Qaiumzadeh, L. Baldrati, J. Cramer, A. Brataas, R. A. Duine, and M. Kläui, Tunable long-distance spin transport in a crystalline antiferromagnetic iron oxide, *Nature* **561**, 222–225 (2018).
- [5] A. Ross, R. Lebrun, O. Gomonay, D. A. Grave, A. Kay, L. Baldrati, S. Becker, A. Qaiumzadeh, C. Ulloa, G. Jakob, F. Kronast, J. Sinova, R. Duine, A. Brataas, A. Rothschild, and M. Kläui, Propagation length of antiferromagnetic magnons governed by domain configurations, *Nano Lett.* **20**, 306 (2020), pMID: 31809058, <https://doi.org/10.1021/acs.nanolett.9b03837>.
- [6] A. Ross, R. Lebrun, C. Ulloa, D. A. Grave, A. Kay, L. Baldrati, F. Kronast, S. Valencia, A. Rothschild, and M. Kläui, Structural sensitivity of the spin hall magnetoresistance in antiferromagnetic thin films, *Phys. Rev. B* **102**, 094415 (2020).
- [7] H. Meer, O. Gomonay, A. Wittmann, and M. Kläui, Antiferromagnetic insulatronics: Spintronics in insulating 3d metal oxides with antiferromagnetic coupling, *Appl. Phys. Lett.* **122**, 10.1063/5.0135079 (2023), 080502, https://pubs.aip.org/aip/apl/article-pdf/doi/10.1063/5.0135079/16715759/080502_1_online.pdf.
- [8] Y. Cheng, S. Yu, M. Zhu, J. Hwang, and F. Yang, Electrical switching of tristate antiferromagnetic néel order in α -Fe₂O₃ epitaxial films, *Phys. Rev. Lett.* **124**, 027202 (2020).
- [9] E. Cogulu, N. N. Statuto, Y. Cheng, F. Yang, R. V. Chopdekar, H. Ohldag, and A. D. Kent, Direct imaging of electrical switching of antiferromagnetic néel order in α -Fe₂O₃ epitaxial films, *Phys. Rev. B* **103**, L100405 (2021).
- [10] H. Jani, J.-C. Lin, J. Chen, J. Harrison, F. Maccherozzi, J. Schad, S. Prakash, C.-B. Eom, A. Ariando, T. Venkatesan, and P. G. Radaelli, Antiferromagnetic half-skyrmions and bimerons at room temperature, *Nature* **590**, 74 (2021).
- [11] F. J. Morin, Magnetic susceptibility of α -Fe₂O₃ and α -Fe₂O₃ with added titanium, *Phys. Rev.* **78**, 819 (1950).
- [12] T. Danegger, A. Deák, L. Rózsa, E. Galindez-Ruales, S. Das, E. Baek, M. Kläui, L. Szunyogh, and U. Nowak, Magnetic properties of hematite revealed by an ab initio parameterized spin model, *Phys. Rev. B* **107**, 184426 (2023).
- [13] A. Ross, R. Lebrun, L. Baldrati, A. Kamra, O. Gomonay, S. Ding, F. Schreiber, D. Backes, F. Maccherozzi, D. A. Grave, A. Rothschild, J. Sinova, and M. Kläui, An insulating doped antiferromagnet with low magnetic symmetry as a room temperature spin conduit, *Appl. Phys. Lett.* **117**, 242405 (2020), <https://doi.org/10.1063/5.0032940>.
- [14] G. A. Acket and J. Volger, Electric transport in n-type Fe₂O₃, *Physica* **32**, 1543 (1966).
- [15] K. Vlasov, E. A. Rosenberg, A. G. Titova, and Y. M. Yakovlev, Hall effect in hematite single crystals in the region of the morin transition, *Sov. Phys.-Solid State* **22**, 967–969 (1980).
- [16] S. V. Ovsyannikov, N. V. Morozova, A. E. Karkin, and V. V. Shchennikov, High-pressure cycling of hematite Fe₂O₃: Nanostructuring, in situ electronic transport, and possible charge disproportionation, *Phys. Rev. B* **86**, 205131 (2012).
- [17] B. Zhao, T. C. Kaspar, T. C. Droubay, J. McCloy, M. E. Bowden, V. Shutthanandan, S. M. Heald, and S. A.

- Chambers, Electrical transport properties of ti-doped $\text{Fe}_2\text{O}_3(0001)$ epitaxial films, *Phys. Rev. B* **84**, 245325 (2011).
- [18] R. Bhowmik and A. G. Lone, Electric field controlled magnetic exchange bias and magnetic state switching at room temperature in ga-doped $\alpha\text{-Fe}_2\text{O}_3$ oxide, *J. Magn. Magn. Mater.* **462**, 105 (2018).
- [19] A. J. E. Rettie, W. D. Chemelewski, B. R. Wygant, J. Lindemuth, J.-F. Lin, D. Eisenberg, C. S. Brauer, T. J. Johnson, T. N. Beiswenger, R. D. Ash, X. Li, J. Zhou, and C. B. Mullins, Synthesis, electronic transport and optical properties of si: $\alpha\text{-Fe}_2\text{O}_3$ single crystals, *J. Mater. Chem. C* **4**, 559 (2016).
- [20] E. Gharibi, A. Hbika, B. Dupre, and C. Gleitzer, Cheminform abstract: Electrical properties of pure and titanium-doped hematite single crystals, in the basal plane, at low oxygen pressure., *Chem. Inform.* **21** (1990), <https://onlinelibrary.wiley.com/doi/pdf/10.1002/chin.199043022>.
- [21] T. R. Paudel, A. Zakutayev, S. Lany, M. d’Avezac, and A. Zunger, Doping rules and doping prototypes in a2bo4 spinel oxides, *Advanced Functional Materials* **21**, 4493 (2011), <https://onlinelibrary.wiley.com/doi/pdf/10.1002/adfm.201101439>.
- [22] J. Robertson and S. J. Clark, Limits to doping in oxides, *Phys. Rev. B* **83**, 075205 (2011).
- [23] H. Pan, X. Meng, D. Liu, S. Li, and G. Qin, (ti/zr,n) codoped hematite for enhancing the photoelectrochemical activity of water splitting, *Phys. Chem. Chem. Phys.* **17**, 22179 (2015).
- [24] J. Sinova, S. O. Valenzuela, J. Wunderlich, C. H. Back, and T. Jungwirth, Spin hall effects, *Rev. Mod. Phys.* **87**, 1213 (2015).
- [25] L. Wang, K. Shen, S. S. Tsirkin, T. Min, and K. Xia, Crystal-induced transverse current in collinear antiferromagnetic $\gamma\text{-femn}$, *Appl. Phys. Lett.* **120**, 012403 (2022), <https://doi.org/10.1063/5.0069504>.
- [26] J. Kipp, K. Samanta, F. R. Lux, M. Merte, D. Go, J.-P. Hanke, M. Redies, F. Freimuth, S. Blügel, and M. Ležaić, The chiral hall effect in canted ferromagnets and antiferromagnets, *Commun. Phys.* **4**, 10.1038/s42005-021-00587-3 (2021).
- [27] L. Šmejkal, R. González-Hernández, T. Jungwirth, and J. Sinova, Crystal time-reversal symmetry breaking and spontaneous hall effect in collinear antiferromagnets, *Sci. Adv.* **6**, eaaz8809 (2020), <https://www.science.org/doi/pdf/10.1126/sciadv.aaz8809>.
- [28] L. Šmejkal, J. Sinova, and T. Jungwirth, Beyond conventional ferromagnetism and antiferromagnetism: A phase with nonrelativistic spin and crystal rotation symmetry, *Phys. Rev. X* **12**, 031042 (2022).
- [29] R. Shindou and N. Nagaosa, Orbital ferromagnetism and anomalous hall effect in antiferromagnets on the distorted fcc lattice, *Phys. Rev. Lett.* **87**, 116801 (2001).
- [30] L. Šmejkal, Y. Mokrousov, B. Yan, and A. H. MacDonald, Topological antiferromagnetic spintronics, *Nat. Phys.* **14**, 242–251 (2018).
- [31] Z. Feng, X. Zhou, L. Šmejkal, L. Wu, Z. Zhu, H. Guo, R. González-Hernández, X. Wang, H. Yan, P. Qin, X. Zhang, H. Wu, H. Chen, Z. Meng, L. Liu, Z. Xia, J. Sinova, T. Jungwirth, and Z. Liu, An anomalous hall effect in altermagnetic ruthenium dioxide, *Nature Electronics* **5**, 735 (2022).
- [32] K. Samanta, M. Ležaić, M. Merte, F. Freimuth, S. Blügel, and Y. Mokrousov, Crystal hall and crystal magneto-optical effect in thin films of srruo3, *J. Appl. Phys.* **127**, 213904 (2020), <https://doi.org/10.1063/5.0005017>.
- [33] D.-F. Shao, J. Ding, G. Gurung, S.-H. Zhang, and E. Y. Tsymlal, Interfacial crystal hall effect reversible by ferroelectric polarization, *Phys. Rev. Appl.* **15**, 024057 (2021).
- [34] K. Fabian, P. Robinson, S. A. McEnroe, F. Heidebach, and A. M. Hirt, Experimental study of the magnetic signature of basal-plane anisotropy in hematite, in *The Earth’s Magnetic Interior*, edited by E. Petrovský, D. Ivers, T. Harinarayana, and E. Herrero-Bervera (Springer Netherlands, Dordrecht, 2011) pp. 311–320.
- [35] Supplemental material, [http://\[publisherwillinsertURL\]](http://[publisherwillinsertURL]) (2023), see Supplemental Material for a comprehensive account of the fabrication procedures and sample quality.
- [36] D. A. Grave, H. Dotan, Y. Levy, Y. Piekner, B. Scherrer, K. D. Malviya, and A. Rothschild, Heteroepitaxial hematite photoanodes as a model system for solar water splitting, *J. Mater. Chem. A* **4**, 3052 (2016).
- [37] D. S. Perloff, Four-point sheet resistance correction factors for thin rectangular samples, *Solid State Electron.* **20**, 681 (1977).
- [38] A. Morrish, *Canted Antiferromagnetism: Hematite* (World Scientific, 1994).
- [39] K. D. Malviya, H. Dotan, D. Shlenkevich, A. Tsyganok, H. Mor, and A. Rothschild, Systematic comparison of different dopants in thin film hematite ($\alpha\text{-Fe}_2\text{O}_3$) photoanodes for solar water splitting, *J. Mater. Chem. A* **4**, 3091 (2016).
- [40] O. M. Lemine, M. Sajieddine, M. Bououdina, R. Msalam, S. Mufti, and A. Alyamani, Rietveld analysis and mössbauer spectroscopy studies of nanocrystalline hematite $\alpha\text{-Fe}_2\text{O}_3$, *J. Alloys Compd.* **502**, 279 (2010).
- [41] J. O. Artman, J. C. Murphy, and S. Foner, Magnetic anisotropy in antiferromagnetic corundum-type sesquioxides, *Phys. Rev.* **138**, A912 (1965).
- [42] I. Dzyaloshinsky, A thermodynamic theory of “weak” ferromagnetism of antiferromagnetics, *J. Phys. Chem. Solids* **4**, 241 (1958).
- [43] P. J. Besser, A. H. Morrish, and C. W. Searle, Magnetocrystalline anisotropy of pure and doped hematite, *Phys. Rev.* **153**, 632 (1967).
- [44] S. Foner, High-field antiferromagnetic resonance in Cr_2O_3 , *Phys. Rev.* **130**, 183 (1963).
- [45] L. Šmejkal, A. H. MacDonald, J. Sinova, S. Nakatsuji, and T. Jungwirth, Anomalous hall antiferromagnets, *Nature Reviews Materials* **7**, 482 (2022).
- [46] H. Meer, O. Gomonay, C. Schmitt, R. Ramos, L. Schnitzspan, F. Kronast, M.-A. Mawass, S. Valencia, E. Saitoh, J. Sinova, L. Baldrati, and M. Kläui, Strain-induced shape anisotropy in antiferromagnetic structures, *Phys. Rev. B* **106**, 094430 (2022).
- [47] H. Ebert, D. Ködderitzsch, and J. Minár, Calculating condensed matter properties using the kkr-green’s function method—recent developments and applications, *Reports on Progress in Physics* **74**, 096501 (2011).
- [48] V. P. Amin, J. Li, M. D. Stiles, and P. M. Haney, Intrinsic spin currents in ferromagnets, *Phys. Rev. B* **99**, 220405 (2019).
- [49] Y. Ayino, P. Xu, J. Tigre-Lazo, J. Yue, B. Jalan, and V. S. Pribiag, Ferromagnetism and spin-dependent transport at a complex oxide interface, *Phys. Rev. Mater.* **2**, 031401 (2018).